

Short communication

## Optical filtering removes non-homogenous illumination artifacts in optical imaging

Andrzej W. Przybyszewski<sup>a,\*</sup>, Takayuki Sato<sup>b</sup>, Mitsuhiro Fukuda<sup>b</sup>

<sup>a</sup> Laboratory for Cortical Organization and Systematics, Brain Science Institute, RIKEN, 2-1 Hirosawa, Wako-shi, Saitama 351-0198, Japan

<sup>b</sup> Laboratory for Integrative Neural System, Brain Science Institute, RIKEN, 2-1 Hirosawa, Wako-shi, Saitama 351-0198, Japan

Received 8 March 2007; received in revised form 7 August 2007; accepted 7 September 2007

### Abstract

Under constant light illumination, cortical neuronal activity slightly modulates intensity of the light reflected from cortical surface. Optical imaging of the reflected light from the cortex has now become a popular method to obtain cortical functional maps. Since the modulation signal is small, this method is very sensitive to other sources of the light intensity changes. A well-known artifact in this signal is the bias in the reflected light intensity due to the curvature of the cortex. The curvature of the cortex creates inhomogeneity in reflected light intensity with characteristic concentric-ring pattern in the functional maps (known as ring-shape artifact). It is particularly visible in single-condition maps if the number of trials is small.

We demonstrate a method that can remove this and similar artifacts using an optical filter to equalize the reflected light intensity. Functional images recorded with the application of our filter – inserted into the optics between the cortex and the camera – became more uniform and distortion-free.

Our approach consisting of the equalization optical filter is appropriate for experiments where inhomogeneous light reflection, single-condition maps, and a small number of trials exist, e.g. imaging studies of higher cortices in behaving monkeys.

© 2007 Elsevier B.V. All rights reserved.

**Keywords:** Intrinsic signal; Ocular dominance column; Orientation column; Cortex; CBV; Cellular swelling

### 1. Introduction

Optical intrinsic signal imaging (OISI) is based on the fact that changes in the activity of local population neurons alter light absorption by the tissue (Blasdel and Salama, 1986; Bonhoeffer and Grinvald, 1996). The data analysis is performed once the digital images have been obtained from the camera. The camera is an intermediate step that converts the analog light signal (reflected light) into a digital image using an analog-to-digital (A/D) converter. To prevent saturation, the A/D converter must have a dynamic range greater than the range of the analog signal. The range of the analog signal for non-uniform light intensity is higher than that for uniform light. Also, the grayscale-resolution is inversely related to the range of the analog signal. The curvature of the cortex introduces

changes in the reflected light intensity and therefore makes it non-uniform. As a result, the reflected light intensity suffers from poor grayscale-resolution upon digitization. Furthermore, the reflected light intensity is only modulated if the number of trials is small or single-condition experimental design (i.e., test images vs. control images) is used, ring-shaped artifact will be present and distort activation patterns in the images. In the present paper, we describe a novel method to remove static inhomogeneity in the reflected light intensity by means of an optical filter. As an example, we employ the optical filter to remove ring-shaped artifacts from the functional columnar maps.

### 2. Material and methods

#### 2.1. Animal preparations

OISI was performed on three hemispheres in two Rhesus monkeys (*Macaca mulatta*). These animals had been used previously for OISI from the inferotemporal cortex. The surgery and recording procedures have been described in detail in a previous study (Li et al., 2003). Briefly, paralyzed monkey (vecuronium

\* Corresponding author at: Department of Psychology, McGill University, 1205 Dr. Penfield Avenue, Montreal, QC H3A 1B1, Canada.

Tel.: +1 514 398 6151; fax: +1 514 398 3255.

E-mail address: przy@ego.psych.mcgill.ca (A.W. Przybyszewski).

bromide; 0.1 mg/(kg h), i.v.) was ventilated with isoflurane in a mixture of 70% N<sub>2</sub>O and 30% O<sub>2</sub>. Craniotomy and duratomy were carried out inside an implanted chamber to expose the cortical surface. EEG was monitored to maintain a proper anesthetic level throughout the experiments. The temperature was maintained  $37.8 \pm 0.2$  °C, and end-tidal CO<sub>2</sub>  $4.5 \pm 0.5\%$ . All experimental procedures were done in accordance with the guidelines of the RIKEN Institute.

## 2.2. Visual stimuli

During the stimulus-on period, one of the four moving oriented square-wave gratings (1–3 cycle/degree;  $0.5^\circ \text{ s}^{-1}$ ; white: 8 cd/m<sup>2</sup>, black: 0 cd/m<sup>2</sup>; 0°, 45°, 90°, or 135°) was presented for 2 s to one eye by using eye shutters. As a control (no stimulation) OISI was recorded when both eye shutters were closed. Altogether, there was one control stimulus trial as described above, and eight test stimulus trials with four different orientations. We will refer to a ‘trial’ as one stimulus epoch (i.e., 1 s pre-stimulus period plus 3 s post-stimulus period).

## 2.3. Imaging systems

### 2.3.1. Optics

Modified tandem-lens optics was used for this study (Fig. 1). An optical filter was placed in the first imaging plane of the

lower tandem-lens (50 mm, f1.2, Nikon) and the charge coupled device (CCD) camera was placed in the second imaging plane of the upper tandem-lens (25 mm, f0.95, CCTV, Japan). Without the filter, the modified system works similarly to the standard tandem-lens optics. Optical filters were designed separately for each region-of-interest (ROI) of the cortex (Fig. 2A). The filter was made by inverting light intensity image of the cortex that would equalize the reflected light intensity. The camera was focused at the location below the cortical surface from where the intrinsic signal was recorded. A single frame image at this depth was taken (Fig. 2B), saved and processed by Photoshop (Adobe) software, where its intensity was inverted. The inverted image with adjusted mean light intensity on Photoshop was printed in the scale 1:1 on a transparency. This transparency formed the optical filter. An example of the optical filter image is shown in Fig. 2C. In the next step, the filter was placed in the filter frame and inserted into the filter positioner to move into an appropriate *x*-, *y*-, and *z*-position, and another picture of the cortex through the filter was taken (Fig. 2D). The filter must fit the image of the cortex precisely to compensate for the static inhomogeneity in the reflected light. This was achieved by moving the filter in the *x*- and *y*-direction in such way that when pial vascular patterns on the cortex matched those on the filter, the pial vasculatures patterns become invisible in the acquired image. Moving the filter in *z*-direction changes the position of the filter relative to

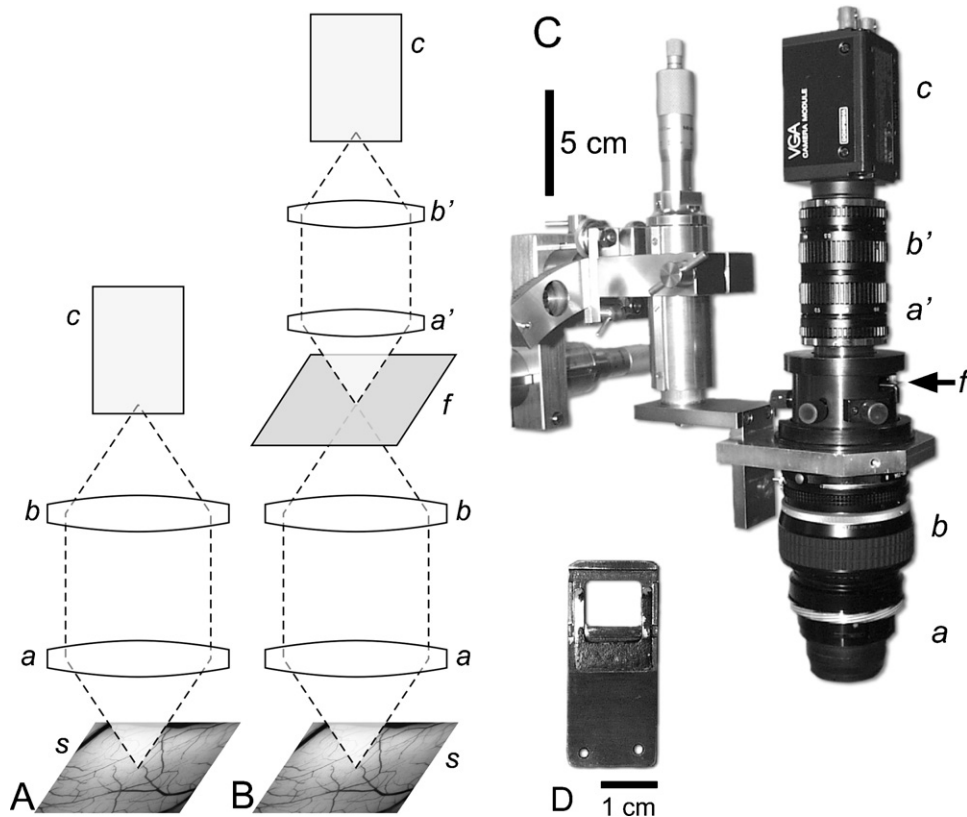


Fig. 1. Commonly used tandem-lens optics for OISI vs. modified optics with the photography of the modified system. (A) Schematics of tandem-lens between cortex and camera in the standard recording system. (B) Schematics of lens and filters between cortex and camera in the modified recording system. The filter was placed in the position of the camera in A, and another tandem-lens system was built between filter and the camera. Abbreviations: s, cortical surface; a and a', objective lenses; b and b', projection lenses; c, CCD camera; f, optical filter. (C) The modified lens system with the CCD camera attached to the micromanipulator. In order to decrease system size, in the set between filter and camera a smaller size lenses were used. (D) Frame with the window for the filter.

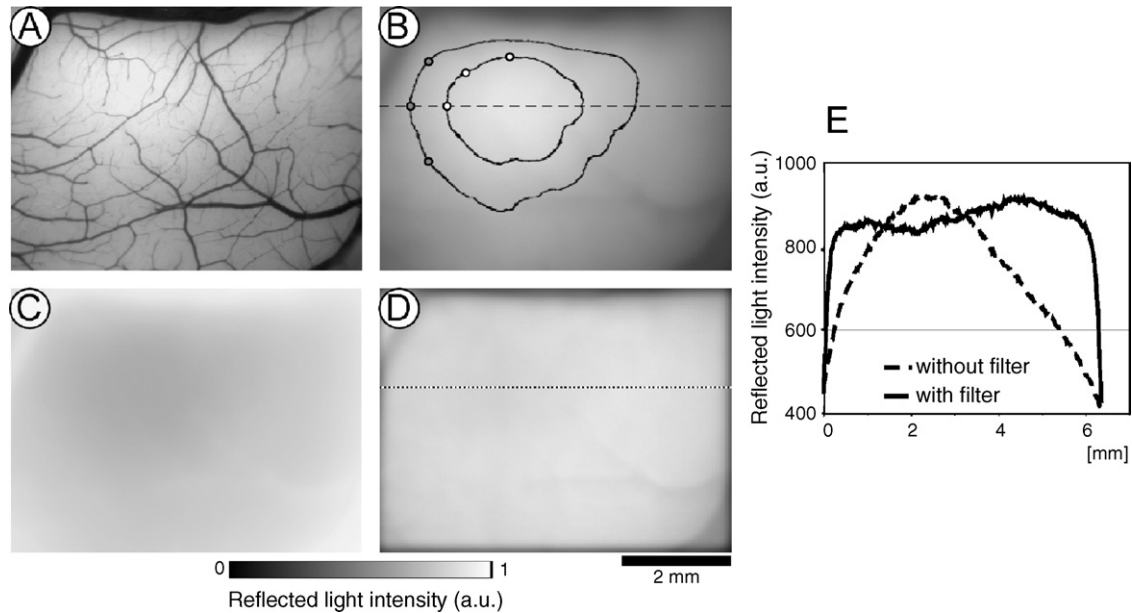


Fig. 2. The correction of inhomogeneity of reflected light intensity with the optical filter. (A) Cortical surface image (green, 540 nm wavelength light illumination). (B) Image of the cortex at the depth of 700  $\mu\text{m}$  below the surface (607 nm illumination); maximum changes in the light intensity are near the upper left corner of the image. Along dotted line intensity profile was analyzed and presented on panel E. Colored dots representing the ring-shape artifacts were added to this image in the same location as in Fig. 4A–C. When dots with the same color were connected, they determined equiluminance rings showed in the image. (C) Image of the filter that was created by inversion of the cortical image (compare to B). (D) Image of the cortex with the filter (compare to B). Along dotted line intensity profile was analyzed and presented in panel E, a.u.: arbitrary unit. (E) Comparisons of light intensity profiles with and without an optical filter (dotted line). A profile of the cortical image taken without filter along the line shown in part B (solid line). A profile of the cortical image taken with filter along the line shown in panel D. (For interpretation of the references to color in this figure legend, the reader is referred to the web version of the article.)

the focal plane. It blurs the image or introduces a low-pass spatial frequency filtering which is necessary to remove the texture of the filter. The adjustments of the filter position are necessary for the functioning of the system. The image intensity of the cortex became more uniform as a result of the static artifacts compensation (compare Fig. 2B and D).

### 2.3.2. Optical intrinsic signal imaging

The exposed cortical surface was illuminated using light of wavelength of either  $540 \pm 10$  nm (pial vessel image) or  $607 \pm 10$  nm (OISI). Images were obtained using a CCD camera ( $640 \times 480$  pixels; CS8310, Teli, Japan) and digitized with a 10-bit video A/D converter board (Pulsar, Matrox Graphics Inc., Canada) connected to the PCI bus of IBM PC. The area imaged was  $6.4 \text{ mm} \times 4.8 \text{ mm}$  and after spatial averaging of the pixels ( $2 \times 2$  binning), it contained  $320 \times 240$  pixels. For the OISI recording, the focusing depth was adjusted to 700  $\mu\text{m}$  below the cortical surface rather than 300  $\mu\text{m}$  commonly used for optical imaging of intrinsic signal. The purpose of imaging the cortical surface out-of-focus is to mitigate the artifact from pial vessels in the generated maps (Bonhoeffer and Grinvald, 1993). Empirically, we have learned that the 300  $\mu\text{m}$  in contrast to 700  $\mu\text{m}$  out-of-focus is frequently not sufficient to avoid pial vessel artifact in differential maps. The differential maps obtained at 0–1000  $\mu\text{m}$  are essentially the same except for the vessel artifacts. We did not systematically study relationships between appearance of ring-shaped artifacts and focal plane. As long as the global inhomogeneity of the reflected

light intensity is present, the ring-shape artifacts will also be observed.

The data acquisition started at a certain phase of respiration in synchrony with heartbeat and continued for 4 s for each stimulus (one trial). Each image was acquired at the rate of 0.5 s per image. Stimulus-on period started 1 s after the onset of data acquisition and continued for 2 s. Inter-stimulus intervals (stimulus offset to onset) were set to 8 s. The period of illumination was restricted to 8 s by a mechanical shutter that opened 2 s before the data acquisition. For each oriented grating, stimulus was presented 20 times to each eye; thus altogether each eye was stimulated 80 times.

### 2.4. Data analysis

A pre-stimulus baseline image was obtained by averaging images taken during 1-s period just before the stimulus started. The percent signal change (first frame analysis) was done by dividing the difference images (stimulus images minus the pre-stimulus baseline image) by the pre-stimulus baseline image (Bonhoeffer and Grinvald, 1996). The resulting percentage signal change for each image (during 2.5 s including 0.5 s delay after the stimulus onset) was then averaged to obtain a single-condition activity map for each stimulus (i.e., four orientations and one blank for each eye).

Below, we will define: single-condition ocular dominance map and differential ocular dominance map, which were used in our analysis. Single-condition ocular dominance map was

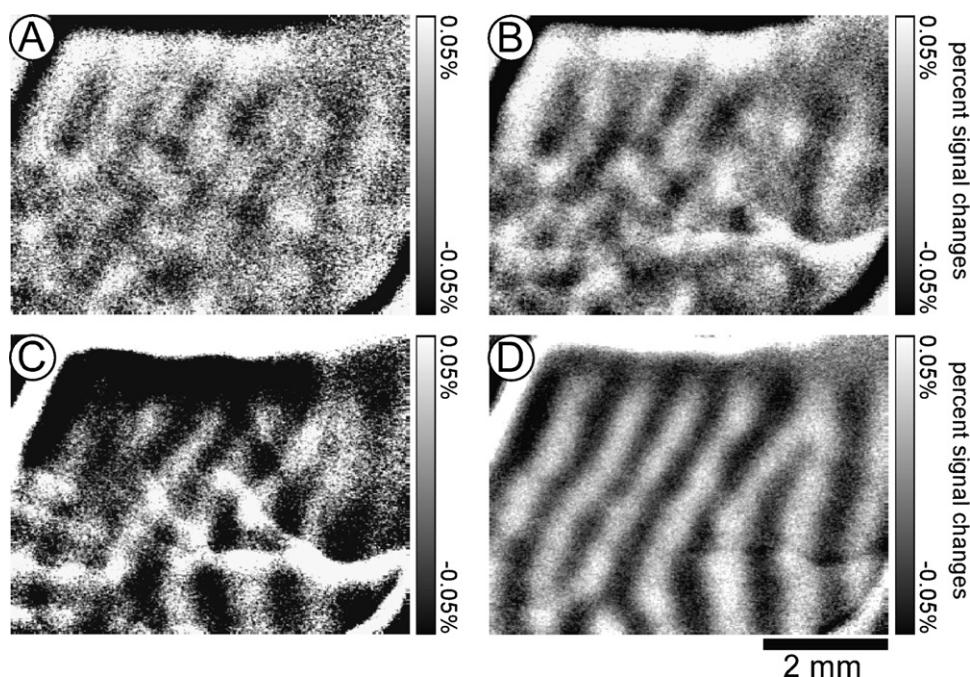


Fig. 3. Comparisons between single-condition ocular dominance map and differential ocular dominance map without optical filter. (A) Averaged single-condition ocular dominance map of the first eight trials during left eye stimulation. Notice ring-shaped artifacts around maximum intensity of illumination. (B) Averaged single-condition ocular dominance map of 80 trials during left eye stimulation. (C) Averaged differential ocular dominance map of the first eight trials obtained by subtracting the responses to left eye stimulation from those to the right eye stimulation. (D) Averaged differential ocular dominance map of 80 trials.

calculated for each eye by subtracting the single-condition activity map for blank stimulus from the averaged single-condition activity map for four-orientation stimulation. Differential ocular dominance map was calculated by subtracting the single-condition ocular dominance map of one eye from that of the other eye.

A Gaussian band-pass spatial filter (cutoff frequencies were  $20.4 \text{ mm}^{-1}$  for the high and  $0.3 \text{ mm}^{-1}$  for the low range) was used to enhance the contrast of ocular dominance columns of the single-condition ocular dominance map, the differential ocular dominance map and a single-condition activity map for one orientation shown in Fig. 4C. Notice that the ring-shaped artifacts are in the narrow frequency range between 5 and 10 cycle/mm and therefore, they are not affected by the Gaussian band-pass spatial filter (Malonek and Grinvald, 1996). Pixels with the same luminance intensity were extracted with help of the IDL software and used to draw the contours (see Fig. 2B).

Ring-shaped artifacts were observed in all three hemispheres that were studied. In the following section we will present experimental results obtained from one hemisphere, in which the ring-shaped artifacts were most clearly visible.

### 3. Results

To examine the ring-shaped artifacts, we performed OISI using the conventional tandem of the optical lens (see Fig. 1A). A curved surface of the cortex introduced inhomogeneity in the reflected light from the ROI (see Fig. 2B). In the single-condition ocular dominance map, obtained by averaging the responses from eight trials (Fig. 3A), ring-shaped artifacts are

clearly visible. These artifacts distort the ocular-dominance-columns pattern and are still noticeable even after averaging the responses from 80 trials (Fig. 3B). However, in the differential ocular dominance map, obtained by averaging the responses from eight trials, the ring-shaped artifacts were not clearly noticeable (Fig. 3C). After averaging the responses from 80 trials, the artifact was completely eliminated (Fig. 3D). It should be noted that ring-shaped artifacts appear to be similarly observed in the control image (not shown). Nevertheless, we have also observed this artifact in the single-condition ocular dominance map.

A more detailed analysis of the images containing the ring-shaped artifacts was performed (Figs. 2 and 4). Red and green markers were placed on the same ring-shaped artifacts in the single-condition ocular dominance map averaged from the eight trials (Fig. 4A). The markers were also placed in the same position in another averaged single-condition ocular dominance map shown in Fig. 4B (eight trials containing clear visible ring-shaped artifacts), and in a single-condition activity map for one orientation (Fig. 4C). The rings seemed to stay nearly at the same positions relative to the markers across different trials. Thus, neither simple averaging of responses nor comparisons of test-stimulus-response and control-stimulus-response seemed to diminish the ring-shaped artifact in functional maps. Dots with the same color turned out to have an identical light level intensity (Fig. 2B). Therefore, we assumed that the ring-shaped artifacts are linked to the inhomogeneity in the light reflected from the cortex.

In order to remove this inhomogeneity we used an optical filter mounted between lenses. Two light intensity profiles

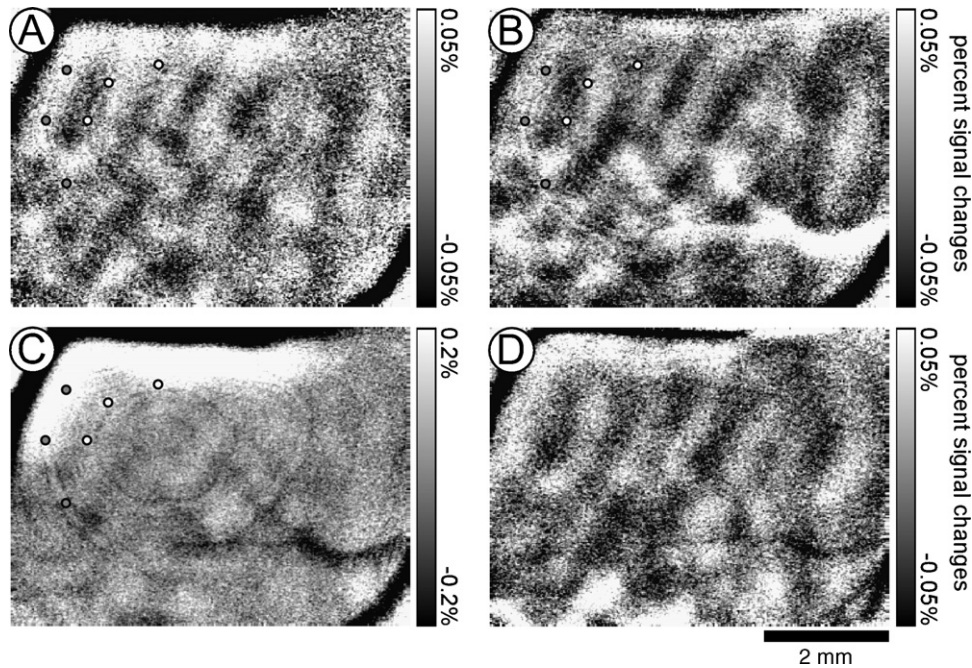


Fig. 4. Consistent appearance of the ring-shaped artifacts removed by introduction of the optical filter. (A) The single-condition ocular dominance map from Fig. 3A with red and green dots placed on two different ring-shaped artifacts. (B) This image is also averaged of the single-condition ocular dominance map, but eight trials with prominent ring-shaped artifacts were selected. Notice that in both images (A and B) ring-shaped artifacts are similar. (C) A single-condition activity map of one-trial recording. This image represents the response to vertical grating. (D) Averaged single-condition ocular dominance map of the first eight trials during left eye stimulation registered in the exactly same conditions as in Fig. 3A but with the optical filter. (For interpretation of the references to color in this figure legend, the reader is referred to the web version of the article.)

of the cortical images are shown in Fig. 2E. The first profile (dotted line) was obtained from a control image recorded without the filter along the dotted line in Fig. 2B. It shows large spatial variability of the intensity. The intensity appears to gradually increase from the peripheral towards the central portion of the image. The second intensity profile (solid line in Fig. 2E) was obtained from the filtered image and along the same line (Fig. 2D). The light intensity profile of the central portion of the filtered image is nearly uniform. Although a considerable decrease in the light intensity is present at the image edge, this affects a relatively small portion of the image area and lies outside the ROI. These differences in intensity profiles strongly influence OISI. The single-condition ocular dominance map obtained by averaging of eight trials (Fig. 3A) was computed in the same experimental conditions but with the optical filter (Fig. 4D). In the last experiment, the ring-shaped artifacts were removed because of the optical filter. We have obtained similar improvements in all three hemispheres in the two monkeys.

#### 4. Discussion

We have showed using a simple example that the optical filter completely removed ring-shaped artifacts caused by global illumination inhomogeneity. This inhomogeneity can be corrected by the division of pre-stimulus image (i.e., first frame analysis, Bonhoeffer and Grinvald, 1996). However, this correction does not diminish ring-shape artifacts as seen in our single-condition maps. Introduction of the optical filter makes

the reflected light intensity profile flat for locations within the boundary of the cortex (central portions of the image). The values of the intensity (central portions of the image) have similar magnitude when compared to the maximum light intensity in the non-filter case (Fig. 2E). For this reason and by direct comparison of the images with and without the filter (data not shown) we think that the intrinsic signal is at least as strong with filter as without. Furthermore, the intrinsic signal is no longer affected by the ring-shape artifact; therefore the ocular dominance map is clearer and more uniform with the filter than without it (Fig. 4). We increased the incident illumination when using the filter so that the CCD camera receives the same reflected light intensity with and without the filter. However, we do not think that an increase in illumination alone could account for the improvement or for the cortex damage because the amplitude of the intrinsic signal is similar with and without the filter (compare Fig. 3A and Fig. 4D).

When observing the ring-shaped artifacts in Fig. 2B and comparing them with the intensity profile (Fig. 2E), we found that these artifacts were observed in the areas with a large gradient of the light intensity. One hypothesis, which could explain the source of the ring-shaped artifacts, is related to the digitization levels of the A/D converter. We used 10-bits A/D converter with 1024 digitization levels. In consequence our converter has precision about 0.1% of the signal amplitude, which is in the same range as our intrinsic signal. Therefore, changes in reflected light intensity due to movements of the cortical surface could introduce abrupt changes in the output signal and in consequence in the optical image. These changes will be more

pronounced in the area with large gradients of the light intensity and they may produce the ring-shaped artifacts. Also the reflected light intensity is influenced by brain movements possibly related to brain volume alterations due to stimulus-induced changes in cerebral blood volume and cellular swelling. In consequence, ring-shaped artifacts are reduced in the differential images but not in the single-condition images. Another possibility is interference of waves reflecting from two non-parallel surfaces. This effect is called Newton's Rings. In this case it is monochromatic light waves that are being reflected at cortical surface and silicon oil. Differences in the refractive index between two different materials (cerebral fluid vs. silicon oil) cause the light wave phase shift. They interact according to the distance between cortical surface and silicon oil. This distance is constantly changing because the convex surface of the cortex.

We have already tested our method in optical imaging from the inferotemporal cortex (see work from our lab: Sato et al., 2004; Uchida et al., 2002). The inferotemporal cortex presents several technical difficulties in the acquisition of intrinsic signals. First, due to the highly skewed shape of the inferotemporal cortex, the reflected light intensity is more inhomogeneous than in the other visual areas. Second, the magnitude of the intrinsic signals is generally smaller in inferotemporal cortex than in V1 cortical region (Tsunoda et al., 2001; Wang et al., 1996; Yamane et al., 2006). Third, in experiments involving the inferotemporal cortex, the patterns of stimulation are more complex (Fujita et al., 1992; Tanaka et al., 1991; Tsunoda et al., 2001) than gratings and "orthogonal" stimulation patterns are not known. Thus, in most cases, test conditions have to be compared with the control (i.e., blank screen); the conditions are similar to Fig. 3A than to Fig. 4C. Also our filter is more effective when applied to the optical imaging where only a small number of trials are possible. For example, when OISI is performed on behaving monkeys (Grinvald et al., 1991; Shtoyerman et al., 2000; Siegel et al., 2003; Vnek et al., 1999), the practical number of trials is significantly less than when anaesthetized animals are used. Furthermore, the intensity profile of the filtered optical image is essentially flat, and therefore, implies that the dynamic range of the analog signal is small. As a result, if the filter is used, the images can be digitized at a high resolution.

### Acknowledgements

We very much appreciate the technical assistance of Dr. Manabu Tanifuji for implementing the modified optics and his

suggested comments on our manuscript. We thank Rahul Chander for his comments and help in editing the manuscript, and Mirosław Jonasz for his suggestions regarding the possible causes of the ring-shaped artifacts.

### References

- Blasdel GG, Salama G. Voltage-sensitive dyes reveal a modular organization in monkey striate cortex. *Nature* 1986;321:579–85.
- Bonhoeffer T, Grinvald A. The layout of iso-orientation domains in area 18 of cat visual cortex: optical imaging reveals a pinwheel-like organization. *J Neurosci* 1993;13:4157–80.
- Bonhoeffer T, Grinvald A. Optical imaging based on intrinsic signals: the methodology. In: Toga AW, Mazziotta JC, editors. *Brain mapping: the methods*. San Diego: Academic; 1996. p. 55–97.
- Fujita I, Tanaka K, Ito M, Cheng K. Columns for visual features of objects in monkey inferotemporal cortex. *Nature* 1992;360:343–6.
- Grinvald A, Frostig RD, Siegel RM, Bartfeld E. High-resolution optical imaging of functional brain architecture in the awake monkey. *Proc Natl Acad Sci USA* 1991;88:11559–63.
- Li H, Fukuda M, Tanifuji M, Rockland KS. Intrinsic collaterals of layer 6 Meynert cells and functional columns in primate V1. *Neuroscience* 2003;120:1061–9.
- Malonek D, Grinvald A. Interactions between electrical activity and cortical microcirculation revealed by imaging spectroscopy: implications for functional brain mapping. *Science* 1996;272:551–4.
- Sato T, Uchida G, Tanifuji M. Nature of neuronal clustering in inferotemporal cortex of Macaque monkey revealed by optical imaging and extracellular recording. *Soc Neurosci Abstr* 2004;34:300–12.
- Shtoyerman E, Arieli A, Slovov H, Vanzetta I, Grinvald A. Long-term optical imaging and spectroscopy reveal mechanisms underlying the intrinsic signal and stability of cortical maps in V1 of behaving monkeys. *J Neurosci* 2000;20:8111–21.
- Siegel RM, Raffi M, Phinney RE, Turner JA, Jando G. Functional architecture of eye position gain fields in visual association cortex of behaving monkey. *J Neurophysiol* 2003;90:1279–94.
- Tanaka K, Saito H, Fukada Y, Moriya M. Coding visual images of objects in the inferotemporal cortex of the macaque monkey. *J Neurophysiol* 1991;66:170–89.
- Tsunoda K, Yamane Y, Nishizaki M, Tanifuji M. Complex objects are represented in macaque inferotemporal cortex by the combination of feature columns. *Nat Neurosci* 2001;4:832–8.
- Uchida G, Fukuda M, Sato T, Tanifuji M. Spike synchronization between functional columns in the inferotemporal cortex of anesthetized monkeys. *Soc Neurosci Abstr* 2002;32, 160-113.
- Vnek N, Ramsden BM, Hung C, Goldman-Rakic PS, Roe AW. Optical imaging of functional domains in the cortex of the awake and behaving monkey. *Proc Natl Acad Sci USA* 1999;96:4057–60.
- Wang G, Tanaka K, Tanifuji M. Optical imaging of functional organization in the monkey inferotemporal cortex. *Science* 1996;272:1665–8.
- Yamane Y, Tsunoda K, Matsumoto M, Phillips AN, Tanifuji M. Representation of the spatial relationship among object parts by neurons in macaque inferotemporal cortex. *J Neurophysiol* 2006;96:3147–56.